Effective slip on textured superhydrophobic surfaces

Salil Gogte, Peter Vorobieff, Richard Truesdell, and Andrea Mammoli
The University of New Mexico, Albuquerque, New Mexico 87131

Frank van Swol
The University of New Mexico, Albuquerque, New Mexico 87131
and Sandia National Laboratories, Albuquerque, New Mexico 87185

Pratik Shah
The University of New Mexico, Albuquerque, New Mexico 87131

C. Jeffrey Brinker
The University of New Mexico, Albuquerque, New Mexico 87131
and Sandia National Laboratories, Albuquerque, New Mexico 87185

(Received 19 November 2004; accepted 28 February 2005; published online 13 April 2005)

We study fluid flow in the vicinity of textured and superhydrophobically coated surfaces with characteristic texture sizes on the order of 10 μm. Both for droplets moving down an inclined surface and for an external flow near the surface (hydrofoil), there is evidence of appreciable drag reduction in the presence of surface texture combined with superhydrophobic coating. On textured inclined surfaces, the drops roll faster than on a coated untextured surface at the same angle. The highest drop velocities are achieved on surfaces with irregular textures with characteristic feature size ~ 8 μm. Application of the same texture and coating to the surface of a hydrofoil in a water tunnel results in drag reduction on the order of 10% or higher. This behavior is explained by the reduction of the contact area between the surface and the fluid, which can be interpreted in terms of changing the macroscopic boundary condition to allow nonzero slip velocity. © *2005 American Institute of Physics*. [DOI: 10.1063/1.1896405]

An interface between a viscous fluid and a solid surface is usually characterized by a no-slip boundary condition, although the notion of possible slip on the boundary was introduced almost 200 years ago.[1] Slip on the boundary can occur on the scale on the order of tens of nanometers,[2–4] but the effects of this phenomenon are not appreciable for macroscopic flows. In countless applications, a limited slip boundary condition would be highly desirable. The motivations include, but are not limited to, drag and pressure drop reduction. Recent advances in materials science have led to creation of superhydrophobic (SH) surfaces with unusual contact properties and motivated new research on the boundary conditions near the latter,[5] although apparently there is no macroscopic slip near SH surfaces produced by application of SH coating to a smooth substrate.

The defining property of SH surfaces is a very high contact angle θ, measured as the angle between the plane of the surface and the tangent to the surface of a droplet resting on it: $\theta > 140°$ [Fig. 1(a)]. We show that in fluid flow near a textured SH surface (e.g., a drop moving down an incline), due to this high θ, the contact area between the fluid and the surface is reduced, producing effective macroscopic slip on scales consistent with the characteristic size of the surface features.

Our basic notion of the flow behavior near a textured SH surface is illustrated in Fig. 1. The characteristic size of the texture is much larger than any surface roughness associated with the SH coating itself, but smaller than the capillary length (2.7 mm for water). The texture can be regular (e.g., grooves) or irregular (random peaks). The direct contact area between the surface and the fluid is limited to the protruding parts of the surface (lands for the regular texture, peaks for the irregular texture), with free fluid surface areas above the depressed parts (grooves for the regular texture, valleys for the irregular texture). We assume that these areas exist because there is insufficient energy to deform the fluid boundary to bring it in contact with all the surface [Fig. 1(a)]. This will lead to a velocity profile in the plane of the lands with zero velocity in the contact area and nearly parabolic velocity distribution in the grooves. A velocity average at the nominal fluid boundary (the plane of the lands) would be greater than zero [Fig. 1(b)]. Similar behavior can be expected for an irregular texture [Fig. 1(c)], although the shape of the real-life boundary of the fluid in the latter case is likely more complicated.

For a flow inside a round pipe with alternating slip/no-slip boundary condition, an analytical solution manifests nontrivial effective slip velocity.[6] For a fixed ratio between the widths of the lands and the grooves, this solution predicts effective slip to increase linearly with the land width. To visualize a plausible velocity distribution near a surface in partial contact with fluid, we conducted a simple finite-element numerical simulation of a Poiseuille flow in a circular cross-section tube with alternating boundary conditions (Fig. 2) for a 1:1 ratio between the widths of the lands (no slip) and the grooves (slip). The simulation shows effective slip increasing with the land width linearly in good agreement with the analytical results.[6] Thus one should expect

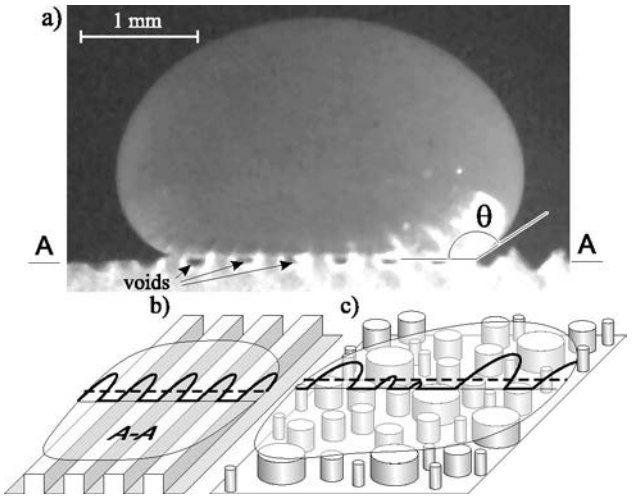

FIG. 1. Schematics of fluid behavior near a superhydrophobic surface: (a) side view of a droplet on regularly grooved surface with voids (no-contact areas) and contact angle θ shown, *A-A* indicates the location of the plane of the nominal fluid boundary, (b) perspective view of the grooved surface showing fluid velocity profile in the *A-A* plane with the dashed line indicating average (i.e., slip) velocity, (c) perspective view of an idealized irregularly textured surface showing the fluid velocity profile and effective slip velocity at the fluid boundary.

macroscopic effective slip velocity to emerge on the boundary as the no-contact areas reach macroscopic size (for water, at least microns).

In real life, the fluid boundary is not perfectly flat, and the patterns shown in Fig. 1 can only be sustained for feature sizes below a certain limit dictated by the capillary length. Moreover, surface deformation in areas above the protruding features (grooves, peaks) is likely to contribute to the overall energy balance of the flow above the surface. Thus one could expect some optimal size for the surface features that maximizes effective slip. An earlier investigation of textured SH surfaces[7] indicates that the pattern of the texture influences the water-repelling properties of the surface, with regular grooved design being optimal for surface drag reduction and maximization of effective slip, as confirmed recently.[8] With these considerations taken into account, we conducted two simple experiments to benchmark the properties of smooth and textured SH surfaces.

In the first experiment, drops move down an inclined surface. The angle of the incline attached to a self-leveling support is measured with a high accuracy (up to 0.5 arc min). 20 cm long samples of materials are placed on the incline. At the elevated end of the sample, a syringe pump dispenses 1.5 mm radius drops. The working fluid is water or a mixture of water and zinc chloride, with a range of densities ρ from 1 g/cc to 1.9 g/cc and a corresponding range of kinematic viscosities ν from 10^{-6} m/s^2 to 10^{-5} m/s^2, the former values corresponding to pure water and the latter to a solution with a 2:1 $ZnCl_2$:water mass ratio. The characteristic Bond number for a water droplet of radius $R=1.5$ mm produced in this arrangement is $\mathrm{Bo}=\rho g R^2/\sigma = 0.30$, where $\sigma=0.0728$ N/m is the surface tension coefficient of water. For a same-size drop of the 2:1 zinc chloride solution, the Bond number is 0.15. Based on the rms velocity of a rolling solid sphere averaged over the extent of the slide for a 2° tilt angle, we estimate the characteristic velocity to be $U_r=9.7$ cm/s. Thus the capillary number for a water droplet is $\mathrm{Ca}=\nu\rho U_r/\sigma=10^{-3}$. The small value of the capillary number indicates that the shape of the droplet is not significantly affected by the motion.[9] The parameters of our experiment are somewhat consistent with the $\mathrm{Bo}\ll 1$ (i.e., surface tension effects dominate gravity effects), $\mathrm{Ca}\ll 1$ assumptions of the theory describing the motion of nonwetting rolling droplets.[9] Our droplet diameter is slightly larger than the capillary length though, so it would be unrealistic to expect good agreement with this theory. For a rolling droplet, the advancing and receding contact angles are not equal. Hysteresis between them for the rolling droplet would be an interesting subject for future study. Reduction of the difference between the advancing and receding angles was reported to make it easier for the droplet to start rolling.[10] The drag reduction due to the emergence of noncontact areas described here, however, should not be directly influenced by the contact angle hysteresis.

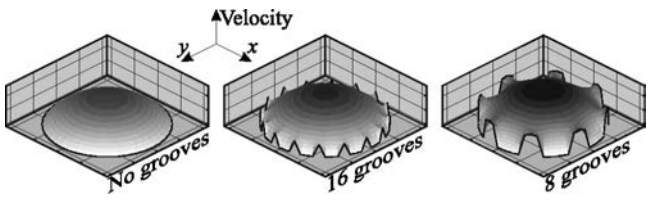

FIG. 2. Velocity distributions obtained by numerical simulation of Poiseuille flow in a circular channel with alternating no-slip and free-surface boundary conditions. Left, uniform no-slip boundary; center, a pattern of 16 lands and 16 grooves of equal width; right, similar pattern with 8 pairs of lands and grooves. Note the increase in maximum flow velocity with groove size.

The second experiment is a study of water flow near a Joukovsky hydrofoil with chord length $L=4.3$ cm, span 3.2 cm, and thickness 25% of the chord. The hydrofoil is installed in a water tunnel at a zero angle-of-attack and attached to a force transducer measuring the drag force. The flow speed U_∞ can be varied to produce a range of Reynolds numbers $\mathrm{Re}=U_\infty L/\nu$ from 1500 to 11 000.

SH coating was prepared by a variation of the low temperature/pressure aerogel thin film process[11] wherein tetraethylorthosilicate was replaced with a 1.0:0.3 molar ratio of tetramethylorthosilicate:trifluoropropyltrimethoxysilane. Drying results in a fractally rough surface terminated with trimethylsilyl and trifluoropropyl ligands. This coating process can be applied to many materials. In the experiments presented here, the materials are limited to sandpaper (aluminum oxide particles on paper substrate) and smooth acrylic polymer. Scanning electron microscope images of the coated acrylic polymer and sandpaper (characteristic feature size 15 μm) are shown in Fig. 3. The thickness of the coating is about half a micron, and on micron and submicron scales the surface features in both cases are fairly similar, including the microcracks.

SH coating applied to a smooth acrylic substrate produces a contact angle of 156° with water. Coated sandpaper has an irregularly textured surface not unlike those considered in Ref. 5. Some preliminary experiments were also con-

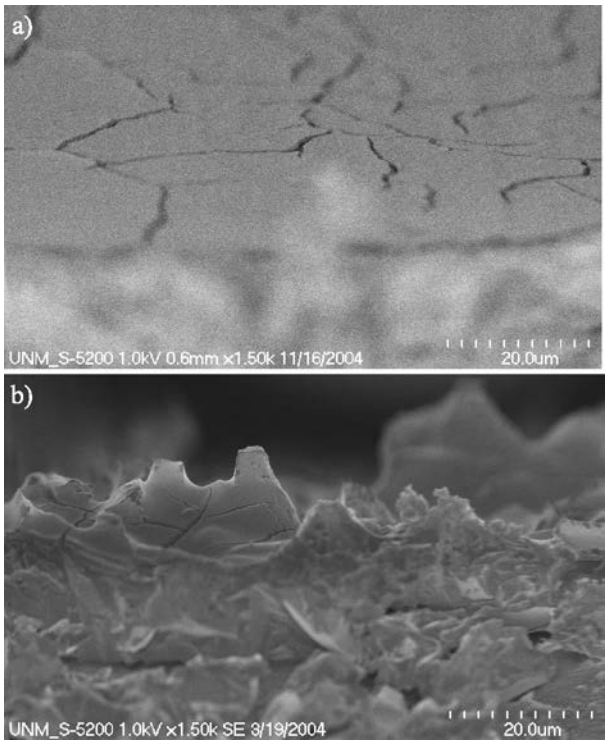

FIG. 3. SEM images of SH-coated surfaces: (a) smooth acrylic polymer, (b) sandpaper (characteristic roughness 15 μm). Note that the submicron surface features produced by the SH coating are much smaller than the substrate roughness in the latter case.

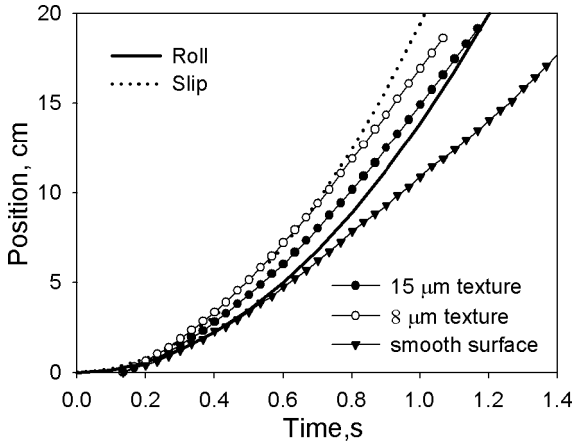

FIG. 4. Ensemble-averaged position of the drop rolling down the SH-coated surface vs time. Plots for each material are labeled in the graph. For reference, graphs for a solid-body rolling and frictionlessly sliding down the incline are also shown.

ducted with grooved SH-coated surfaces. For these, photographs of a drop resting on the surface [Fig. 1(a)] clearly showed alternating contact-no-contact areas, as also previously reported in Ref. 9.

In experiments with the inclined surface, the tilt angle of the incline was varied from 1° to 3°, and a 30 frame-per-second digital video camera (720 by 480 resolution) was mounted at 90° to the plane of the sample. Here we present observations with three types of SH-coated samples: 1200 grit sandpaper (irregular surface texture, characteristic feature size 15 μm), 2400 grit sandpaper (similar texture with feature size 8 μm), and mirror-smooth acrylic substrate. From here on, this surface will be referred to as "untextured" or "smooth," although it still has surface features due to the application of the SH coating. Without the coating, each of the materials is hydrophilic. For each material, at least two samples were coated and mounted on the incline. Video records were analyzed to produce sequences of centerline positions for drops moving down the incline. These sequences were then ensemble averaged for each material type, solution type (pure water, 2:1 $ZnCl_2$:water, etc.), and tilt angle.

Figure 4 shows ensemble-averaged trajectories for water drops, tilt angle 2°. Drops move down surfaces with irregular textures faster than down the untextured surface, suggesting that macroscopic motion of the drops down the textured incline can be interpreted as a combination of rolling and sliding with a nonzero effective slip velocity produced by a mechanism similar to that shown in Fig. 1(d). Not unexpectedly, comparison with the trajectories for the ideal cases of solid-body roll and slide show that the drops are initially moving faster than they would if they were in solid-body rolling mode. Untextured SH-coated surface is characterized by much lower velocities than the textured surfaces, and the drop on this surface reaches a terminal velocity of about 16 cm/s, compared with 25 cm/s for the 15 μm and 26 cm/s for the 8 μm surfaces. Experiments with 1:1 and 2:1 $ZnCl_2$:water solutions show similar results, but with decreasing terminal velocities. The theoretical terminal velocity of the water drop[9] is on the order of meters per second for our parameter values. This disagreement is not surprising: our drops are larger and much less viscous than the glycerol drops for which the terminal velocity results were consistent with the theory.[12]

In hydrofoil experiments, we measure the drag for the following surface types: SH-coated textured surface with 15 μm and 8 μm roughness, the same rough surface without the coating, and coated smooth acrylic surface. Once again, the SH coating of the surface with 8 μm roughness manifests the greatest apparent drag reduction–18% compared with the untextured hydrofoil for Re=1500. This consistency with the droplet experiment is in agreement with our notion of the similar physical mechanism responsible for effective slip velocity in both cases. As Re increases, the drag reduction becomes smaller (7% at Re=11 000). The same textured surface *without* the SH coating is characterized by a several percent *increase* in drag compared with the untextured surface. Figure 5 shows the dependence of drag coefficients of each surface on Re, as well as the percentage of drag reduction for the textured surfaces compared with the untextured surface. Drag coefficient C_D represents the normalized drag force D: $C_D = 2D/(\rho U_\infty^2 S)$, where S is the cross-sectional area of the hydrofoil in the direction of the freestream.

The drag force can be related to the average value of the skin friction coefficient:

$$D \sim A\overline{\tau_w} = A\nu\rho\overline{(\partial U/\partial y)_w}, \tag{1}$$

where A is the hydrofoil surface area, $\overline{(\cdot)}$ denotes averaging over this area, the subscript w indicates the value on the

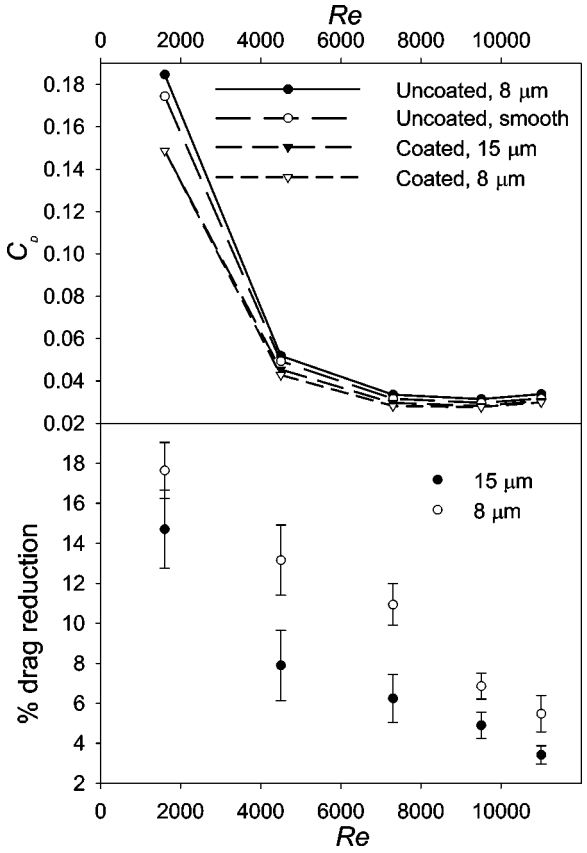

FIG. 5. Top—drag coefficient C_D on a Joukovsky hydrofoil in a water tunnel as the function of Reynolds number for different surface treatments. Curves corresponding to each surface type are labeled in the graph. Bottom—drag reduction for coated textured surfaces compared with smooth surface.

surface (wall), and y is the local coordinate normal to the surface. Usually the boundary of the fluid and the surface coincide. In our case, this condition is violated on the scales commensurate with the characteristic texture size of the SH-coated surface. Equation (1) should still hold on the macroscopic scale that does not resolve the surface features. The actual velocity on the fluid boundary will alternate between zero in contact areas and nonzero in areas above voids [Fig. 1(a)], but on the same macroscopic scale it will average to a nonzero slip velocity U_s.

For the hydrofoil experiments, the ratio U_s/U_∞ can be inferred from the drag reduction. We can estimate the boundary layer thickness δ at mid-chord $x=L/2$ using the Blasius similarity solution for the flat plate.[13] $\delta \sim 5\sqrt{\nu x/U_\infty}$. For the range of the Reynolds numbers we investigated, δ is on the order of 1 mm, large compared with the characteristic scale associated with the surface texture (10 μm). Thus we assume that the boundary layer thickness on the hydrofoil is unaffected by the surface texture and coating. Further we assume that the velocity profile for the textured surface can be related to that for the smooth surface as follows. For the smooth surface $U=0$ at $y=0$; for the textured surface $U=U_s$ at $y=0$, but the shape of the profile of $U-U_s$ in the boundary layer is still described by the same similarity solution as that of U in the smooth surface case. Then from simple geometric considerations it follows that $U_s/U_\infty = 1 - \overline{\tau_{w,t}}/\overline{\tau_{w,s}}$ where the subscripts t and s correspond to the estimates of $\overline{\tau_w}$ for the cases of textured and smooth surface using our drag measurements and Eq. (1). For the best-case scenario (textured SH-coated surface with feature size ~ 8 μm), this slip velocity estimate is 0.5 cm/s for Re $=1500$, $U_\infty = 3.7$ cm/s and 1.4 cm/s for Re $=11\,000$, $U_\infty = 25.6$ cm/s. Overall, the ratio U_s/U_∞ appears to decrease with Re.

The measurements reported here are rather preliminary, and a more thorough study of the combined effects of surface texturing and SH coating on the fluid flows near the surface is certainly warranted. Specifically, measurements of rolling drop and external flow properties near regularly textured (grooved) surfaces would be very interesting. For the external flow, it would also be highly desirable to acquire the velocity profiles in the immediate vicinity of the surface, especially near the leading edge of the hydrofoil, where the boundary layer is the thinnest and where most of the drag accumulates. In this area, the effective slip length might well be on the order of 10% of the boundary layer thickness, which would explain the considerable drag reduction observed. Any future study should also concentrate on determining the optimal size of the surface texture feature to minimize the drag.

This work was supported in part by the U.S. Department of Energy Office of Basic Energy Sciences, Division of Materials Science and Engineering, AFOSR, and by Sandia National Laboratories LDRD program.

[1] C. Navier, "Memoire sur les lois du mouvement des fluids," Memoires de l'Academie Royale des Sciences de l'Institut de France **6**, 389 (1823).
[2] J. Baudry and E. Charlaix, "Experimental evidence for a large slip effect at a nonwetting fluid-solid interface," Langmuir **2001**, 5232.
[3] V. S. J. Craig, C. Neto, and D. R. M. Williams, "Shear-dependent boundary slip in an aqueous Newtonian liquid," Phys. Rev. Lett. **87**, 054504 (2001).
[4] C.-H. Choi, J. A. Westin, and K. S. Breuer, "Apparent slip flows in hydrophilic and hydrophobic channels," Phys. Fluids **15**, 2897 (2003).
[5] Y. Zhu and S. Granick, "Limits of the hydrodynamic no-slip boundary condition," Phys. Rev. Lett. **88**, 106102 (2002).
[6] E. Lauga and H. A. Stone, "Effective slip in pressure-driven Stokes flow," J. Fluid Mech. **489**, 55 (2003).
[7] Z. Yoshimitsu, A. Nakajima, T. Watanabe, and K. Hashimoto, "Effects of surface structure on the hydrophobicity and sliding behavior of water droplets," Langmuir **2002**, 5818.
[8] J. Ou, B. Perot, and J. P. Rothstein, "Laminar drag reduction in microchannels using ultrahydrophobic surfaces," Phys. Fluids **16**, 4635 (2004).
[9] L. Mahadevan and Y. Pomeau, "Rolling droplets," Phys. Fluids **11**, 2449 (1999).
[10] J. Kim and C.-J. Kim, "Nanostructured surfaces for dramatic reduction of flow resistance in droplet-based microfluidics," Proceedings of the IEEE Conference MEMS, Las Vegas, NV, 2002.
[11] S. S. Prakash, C. J. Brinker, and S. M. Rao, "Silica aerogel films prepared at ambient pressure by using surface derivatization to induce reversible drying shrinkage," Nature (London) **374**, 439 (1995).
[12] D. Richard and D. Quéré, "Viscous drops rolling on a tilted non-wettable solid," Europhys. Lett. **48**, 286 (1999).
[13] H. Blasius, "Grenzschichten in Flüssigkeiten mit Kleiner Reibung," Z. Math. Physik, Bd. **56**, 1 (1908).